An Investigation Demonstrating the Feasibility of Microwave Sintering of Base-Metal-Electrode Multilayer Capacitors

Y. FANG,[1] M.T. LANAGAN,[1] D.K. AGRAWAL,[1] G.Y. YANG,[1] C.A. RANDALL,[1] T.R. SHROUT,[1]
A. HENDERSON,[2] M. RANDALL[2] & A. TAJUDDIN[2]

[1]*Center for Dielectric Studies, Materials Research Institute, The Pennsylvania State University, University Park, PA 16802, USA*
[2]*Kemet Electronics Corp, 201 Fairview St. Ext, Fountain Inn, SC 29644-0849, USA*

Abstract.   A microwave sintering technique has been developed for base-metal electrode (BME) multilayer ceramic capacitors (MLCCs). Commercial green chips of size 0603 MLC with nickel electrodes were sintered in a microwave field. With a specially designed susceptor/insulation package to optimize coupling and uniformity of heating, a number of sintering experiments were conducted in the temperature range of 1200 to 1250°C in a multimode microwave cavity operating at 2.45 GHz under a partially reducing atmosphere. Microstructure of the microwave processed MLCCs was investigated with both SEM and TEM techniques. The dielectric properties of the microwave sintered MLCCs were measured and compared with those sintered using conventional process at 1320°C and lower pO_2's $\approx 10^{-9}$ atms. The results demonstrate that nickel electrodes remain metallic after microwave sintering even though the pO_2's were relatively high and would thermodynamically favor NiO. The microwave sintered samples showed a dense, fine and uniform microstructure. The properties of the microwave-sintered samples were comparable to the conventionally sintered samples. The microwave processing was found to have enhanced sintering kinetics of the BME MLCCs, lowering sintering temperature by about 100°C and also the processing time by about 90%.

Keywords: X7R, microwave sintering, multilayer capacitor, base metal electrodes, dielectrics

1. Introduction

Multilayer ceramics capacitors (MLCCs) are important electronic components used in almost all areas of electronics (10^{12} components/year). Major technology drivers are miniaturization, higher capacitive volumetric efficiency, higher reliability, and lower production cost [1–4]. In designing capacitors, the dopants are added to a basic $BaTiO_3$ powder to control temperature coefficient of capacitance, magnitude of dielectric permittivity and limit dielectric loss, maximize insulation resistance, and degradation resistance. Over 80% of modern multilayer capacitors involve the cofiring of the $BaTiO_3$ dielectric formulations with nickel inner electrodes. In order to cofire a dielectric with nickel, firings have to be conducted at a low pO_2, typical firings involve temperatures ~1260 to 1300°C and atmospheres with $pO_2 \approx 10^{-10}$ to 10^{-12} atms. To improve

insulation resistance and degradation resistance, the sintering stage is followed by a reoxidation anneal at $pO_2 \sim 10^{-8}$ atms at ~800°C [5]. This process raises the interfacial barriers at the grain boundaries and reduces the oxygen vacancy concentration in grains, grain boundaries and electrode interfaces [6, 7]. To design $BaTiO_3$ to be able to fulfill all requirements with X7R temperature dependence, there has to be less than ±15% change in capacitance between room temperature values and all temperatures in the range –55°C to 125°C. To obtain this property, dopants are inhomogeneously distributed. In some cases, this can be a core-shell microstructure [8–10]. To ensure high reliability, formulations have to include amphoteric dopants and acceptors. Amphoteric ions involve cations that can occupy either the A- or B-sites of the perovskite structure and act as either a donor or acceptor impurity ion [11–13]. Segregation of the amphoteric ions in the

grain boundary regions with acceptors is an important factor controlling grain boundary resistance, against electronic and ultimately oxygen vacancy conduction. It is the oxygen vacancy redistribution under a direct bias that ultimately controls the insulation resistance degradation rates of the BME capacitors. Limiting the concentration of oxygen vacancies and their mobility is a key part of the strategies used to maximize lifetime against degradation.

Microwave processing of ceramic materials has been widely studied in past twenty years [14–17]. Microwave sintering has been shown to typically enhance the kinetics of densification and also grain growth in some cases [16]. This change in kinetics often leads to differences in microstructure. Earlier microwave sintering studies on electroceramics and devices have involved $Ba(Zn_{1/3}Ta_{2/3})O_3$ (BZT) [18], multilayer ferrite inductors [19], $Pb(Zr,Ti)O_3$ piezoelectric ceramics, ZnO varistors, and air-fired capacitors [20]. BME capacitors are typically more difficult to process with the desired properties and therefore are considered for microwave sintering [21, 22]. One of the attractive points of the microwave sintering is in the fast firing and different mechanisms that drive densification. The objective of this paper is to demonstrate that these differences can give new opportunities in the production of BME multilayer capacitors.

2.   Experimental Procedure

2.1.   Microwave Sintering

The microwave sintering experiments of MLCCs were conducted in a 6 KW, 2.45 GHz multimode microwave furnace with an atmosphere control capability. The samples were encased in a microwave susceptor (ferrite) located in a thermal insulation package on the turntable in the microwave chamber. The temperatures of the samples were monitored with an optical pyrometer (Leeds and Northrup Co., Philadelphia, PA, USA) through a quartz window at the top of the chamber as schematically shown in Fig. 1. This special insulating casket configuration was used to achieve efficient heating and uniform temperature distribution during sintering.

Commercial green chips of X7R MLCCs (size 0603) with nickel internal electrodes and nominal sintered size of 1.52 mm × 0.76 mm × 0.76 mm (0.06″ × 0.03″ × 0.03″) were used for the microwave
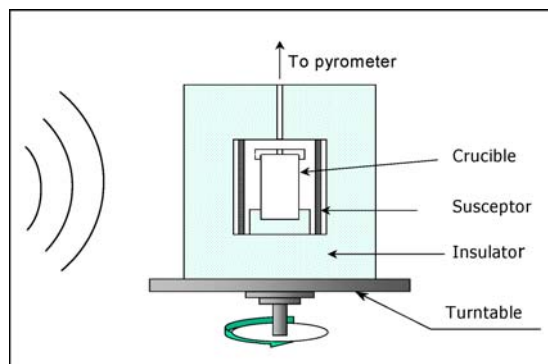

Fig. 1. A schematic diagram of the microwave sintering furnace. Temperatures of the components were monitored through a vertical port directing to an optical pyrometer.

sintering study. Samples were debinded using conditions typically used in mass production and, therefore, details of this process cannot be revealed.

The microwave sintering experiments were carried out in a temperature range of 1200 to 1250°C with an average heating ramp rate of about 25°C/min. The total heating period was 1.5–2 h, including a soak time of approximately 20 minutes at the peak temperature. In order to prevent oxidation of the internal nickel electrodes, an ambient-pressure atmosphere of ultra-high purity nitrogen with less than 1% hydrogen was kept in the microwave chamber during the microwave sintering. The oxygen partial pressure of the atmosphere was approximately 10^{-6} atm. This is a higher partial pressure than used under conventional sintering conditions as it would lead to an oxidation of the nickel electrodes. For comparison, conventional sintering was also conducted but an atmosphere of wet nitrogen containing less than 1% hydrogen ($pO_2 = 1.85 \times 10^{-9}$ atm.) was used. An oxygen sensor is located just above the samples in the tube reactor. The ramping rate in the conventional sintering was kept low to avoid thermal stress. The samples were briefly held at a temperature below 1000°C and at 1320°C for 2 h, respectively. The samples were cooled slowly to room temperature. The conventional firing process took 15 h with a total processing time of about 24 h. Figure 2 shows a comparison of the temperature profiles of both microwave and conventional sintering processes.

2.2.   Characterization

Microstructural and electrical characterization was carried out on the sintered BME MLCCs. Geometric
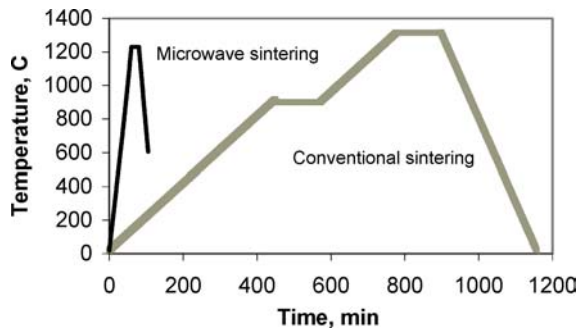
Fig. 2. Radically different profiles for conventional BME firing and microwave firings. Both firings are after a pre-debinding thermal step in a conventional batch furnace.
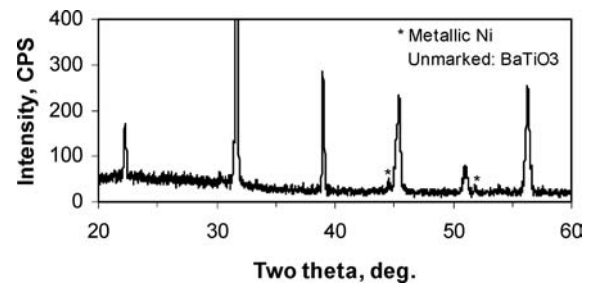

Fig. 3. XRD of the as-sintered end surface of the electrodes of the microwave sintered BME 0603 showing that the Ni electrodes maintained metallic after microwave sintering. The XRD pattern was obtained by scanning the as-sintered surface with the exposed electrodes of an array of 64 chips parallelly aligned.

density of the samples was also measured. In order to initially assess the state of the nickel electrodes (metallic Ni), X-ray diffraction (XRD, Scintag, Sunnyvale, CA) was done on the exposed electrodes of the as-sintered parts (with an array made of a number of MLCC chips aligned in parallel) as well as the bulk powder made from the sintered parts. The microstructure of the microwave-sintered MLCC chips was studied with scanning electron microscopy (SEM, Hitachi 3000S). A selected microwave-sintered sample was also studied with transmission electron microscopy (TEM). Cross-sectional TEM samples of the Ni-BaTiO$_3$ MLCCs were prepared following traditional procedures including polishing and ion milling. Ion milling was performed using an EAF Model 3000 Ion Mill operating at 4–5 kV and 5 mA with an inclination angle of 10–12°. The studies of microstructure and microchemistry of the BME MLCCs were performed using a JEOL transmission electron microscope equipped with a field emission gun (JEOL 2010F) operating at 200 kV. Energy dispersive spectroscopy (EDS) was carried out with the Emispec system in transmission electron microscopy (TEM) mode.

For dielectric property measurements, the microwave-sintered parts were re-oxidized in a conventional furnace. Basic dielectric properties were measured for a number of components that had termination electrodes fired on. Capacitance, tanδ, and insulation resistance were all accessed for both conventional and microwave sintered components. Capacitance and dielectric loss factor as a function of temperature in the range of 140 to −55°C were measured at 100 Hz, 1000 Hz, and 10 kHz on the

re-oxidized microwave-sintered samples (gold plated) and the standard control with the cooling rate at 2°C/min. Highly accelerated life test (HALT) was also carried out on the samples randomly chosen from the selected batches of both microwave and conventional sintering. The samples were terminated with copper, and tested for 92 h at 125°C and 50 V (twice rated voltage).

3. Results and Discussion

The microwave-sintered MLCC chips were found to be uniform, dense, light brown in color, and free from physical flaws, such as delamination or cracking, with geometrical densities up to 5.81 g/cm^3. The conventional samples showed an average geometric density of 5.74 g/cm^3. The results of the characterization are described below.

3.1. State of Internal Electrodes

Besides the matrix perovskite BaTiO$_3$, the X-ray diffraction (XRD) of the as-sintered surface of the microwave sintered samples showed peaks of metallic Ni only (Fig. 3). No evidence of nickel oxide was observed according to XRD study.

3.2. Microstructure

Representative SEM micrographs of the fracture surface and free surface of the microwave-sintered
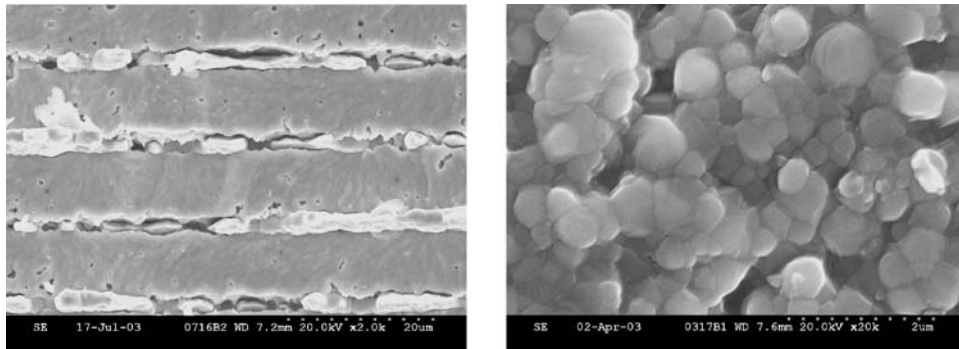
Fig. 4. SEM showing microstructure of the fracture surface and grain size of BME 0603 MLC microwave sintered for 20 min. at 1250°C.
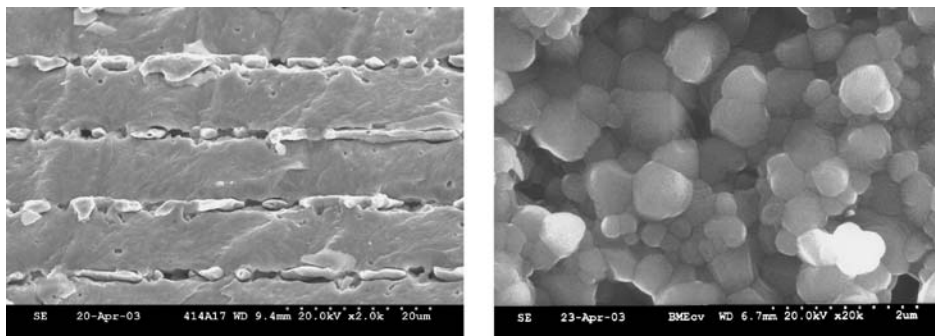

Fig. 5. SEM showing the fracture surface and grain size of the conventionally sintered BME 0603 MLC (900°C/2 h + 1320°C/2 h).

Ni-electrode MLCC chips (cross section) are shown in Fig. 4. Highly dense microstructures were achieved by microwave sintering at about 1250°C. The internal electrodes were found to be continuous. Since the total processing time in the microwave sintering was only about 10% of that in the conventional sintering, the dense microstructures suggest that the densification kinetics of the BME MLCCs was substantially enhanced in the microwave sintering. The average grain size of the microwave-sintered X7R matrix was 0.5–0.6 μm (Fig. 4), similar to that of the conventionally sintered sample (Fig. 5).

Figure 6 shows typical bright-field TEM images of the BaTiO$_3$ in microwave (a) and conventionally (b) sintered Ni-BaTiO$_3$ MLCCs, respectively. In general, the microstructural features of BaTiO$_3$ dielectrics are identical in both capacitors. The microstructure is inhomogeneous through the BaTiO$_3$ dielectric layers. Structural defects are clearly shown in some grains. The defects are associated with local high concentration of oxygen vacancies [1–3]. In addition, the grain boundaries are free of any additional phases.

Figure 7 shows a bright-field image of the interface between the BaTiO$_3$ dielectric and Ni internal electrode. The interface indicated by the arrow in Fig. 7 is free of any oxide phase and is identical with the results obtained with the MLCCs sintered using conventional method. A NiO interfacial layer is expected to form in samples processed at the oxygen partial pressure $\sim$10^{-6} atms in the conventionally sintered BME-MLCCs. The interface without NiO is attributed to the fast co-firing of the MLCCs using microwave method.

3.3. *Dielectric Properties*

The dielectric properties of representative microwave-sintered BME MLCC samples are listed in Table 1. This table compares variation in properties from 50 samples, in terms of device capacitance, dielectric loss at 1 kHz, temperature coefficient at −55°C and 125°C, insulation resistance at 25 and 125°C and breakdown voltage. The samples marked with C were
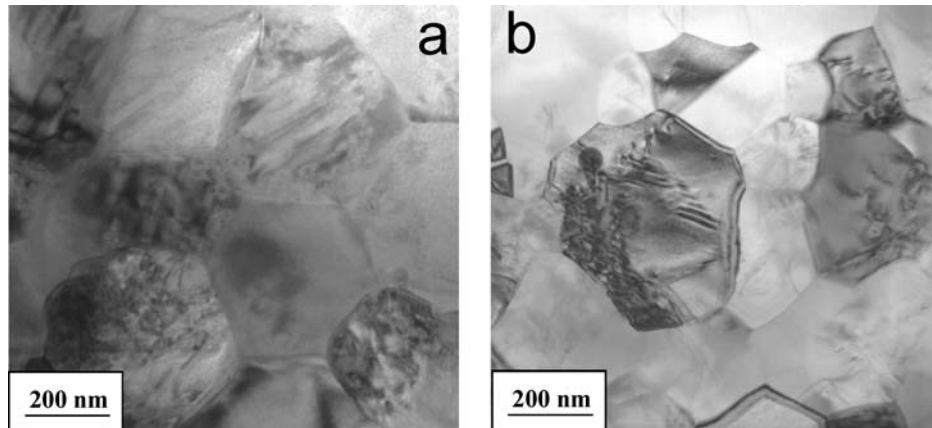
Fig. 6. Typical bright-field TEM images of the BaTiO$_3$ in (a) microwave and (b) conventionally sintered Ni-BaTiO$_3$ MLCCs, respectively.
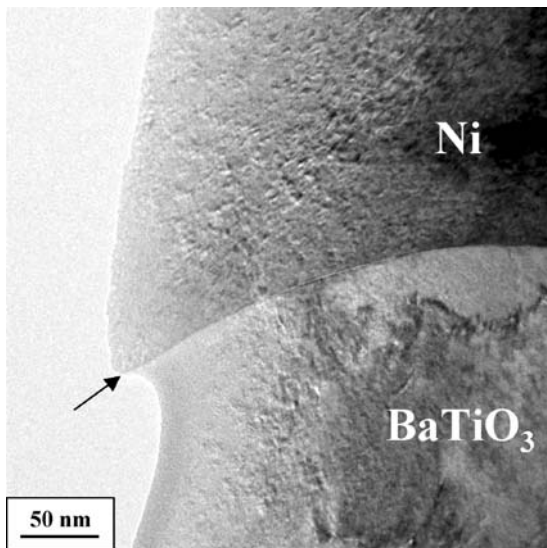

Fig. 7. Nickel-BaTiO$_3$ electrode interface in a microwave fired multiplayer capacitor after re-oxidation.

conventionally sintered, and those marked with M were microwave sintered. All the samples were the same type (size 0603). The standard data were taken from a pusher kiln on these dielectrics and contrasted to the microwave fired samples. Generally, the properties of the microwave-sintered batch were close to that of the control, but standard deviation in some batches and the differences between batches were still large. Since the sintering kinetics was substantially enhanced, microwave processing has a much narrower processing window than the conventional process, thus the process

needs to be much more carefully designed and precisely controlled. Optimization of the processing parameters and the automation of the process will certainly improve the reproducibility of the microwave sintering process and thus the properties of the sintered parts.

Figure 8 shows the capacitance histogram of microwave-fired multilayer capacitor chips measured at 1 kHz. It is seen that the capacitances of all the tested samples are above the nominal of the standard (100 nF). The distribution of capacitance is very narrow. The microwave-sintered BME capacitors showed excellent capacitance and dielectric loss as a function of temperature. Figure 9 shows C and D vs. T curves of a representative microwave-sintered BME sample (Batch M5, Table 1) in comparison with the standard. Both the microwave-sintered sample and the standard showed peak capacitance in the temperature range around room temperature. The capacitance decreased at both low and high temperature ranges. However, in the whole tested temperature range, the microwave-sintered BME capacitor showed significantly higher capacitance than the standard. Dielectric loss of the samples decreased as the temperature increased. In the range between 75 to $-55°$C, the dielectric loss of the microwave-sintered sample was lower than the standard. This indicates that the microwave sintered BME MLCCs have excellent dielectric properties.

Among the 20 parts randomly chosen from a batch microwave sintered at 1250°C for 20 min (M5, Table 1), and same number of parts from a conventionally sintered batch (C2, Table 1), after 92 h at 125°C and 50 V (twice rated voltage), there was no failure or IR degradation in both batches. Sample M4 in

Table 1. Dielectric properties of the microwave and conventionally sintered BME 0603 MLCCs.

No.	Firing conditions	Cap (nF, N = 50)			DF (%)		TC (%)		25°C IR (G-Ω)		125°C IR (G-Ω)		Breakdown voltage (V)		
		Avg.	STD (nF)	STD (%)	Avg.	STD	−55°C	125°C	Avg.	STD	Avg.	STD	Avg.	STD	Min.
C1	Standard	100	3.67	3.66	2.57	0.033	−15.44	−15.10	30.80	0.16	3.81	0.21	924.4	86.0	780
C2	1320°C/120 Min	113	1.76	1.56	2.36	0.014	−13.57	−16.60	23.80	1.48	1.70	0.21	835.0	80.2	700
M1	1225°C/10 Min.	97	3.17	3.28	2.06	0.304	−9.37	−11.45	28.52	0.60	1.68	0.09	660.0	162.6	330
M2	1225°C/20 Min.	92	13.27	14.47	2.10	0.022	−10.12	−12.27	27.45	1.79	1.59	0.16	747.0	46.2	640
M3	1230°C/40 Min.	105	4.73	4.51	2.12	0.044	−9.70	−14.12	29.44	1.60	1.52	0.13	793.0	87.2	690
M4	1250°C/20 Min.*	97	4.25	4.36	3.83	0.681	−17.67	−4.92	25.11	4.98	3.09	0.17	472.0	147.7	108
M5	1250°C/20 Min.	105	1.99	1.90	2.09	0.016	−10.53	−12.89	28.56	0.94	1.78	0.09	817.0	56.6	720
M6	1250°C/30 Min.	100	6.69	6.67	2.27	0.028	−12.10	−11.08	24.93	3.15	1.47	0.14	528.0	190.3	220

*The heating rate in this run was much higher (∼50˚C/min) than others.
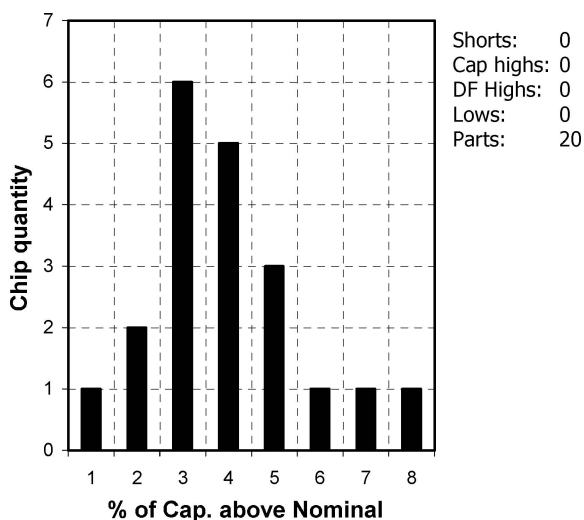

Fig. 8. Histogram of microwave fired multiplayer capacitor chips. Mean capacitance = 104.5 nF with a standard deviation of 1.99 nF, after re-oxidation.

Table 1 (microwave, 1230°C × 40 min) had degradation and failure of 5 out of 8 parts, the remaining 3 did not show any degradation. The degradation of the samples in batch M4 could be caused by thermal stress created due to high heating rates in the microwave processing. Slower heating and cooling in microwave firing improve the quality of the products.

3.4. Process Comparison

Comparison between the microwave and conventional processing conditions (Table 2) shows that, to achieve similar results as the conventional sintering,
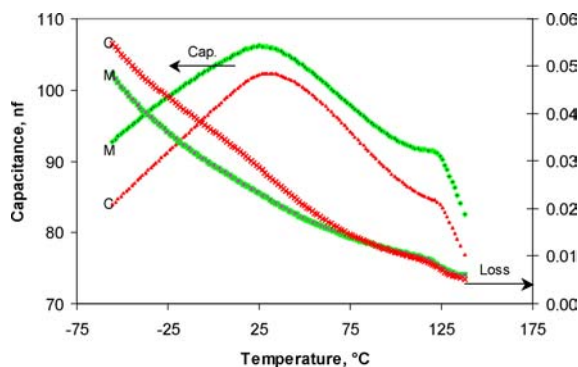

Fig. 9. Comparison of the temperature dependence of the BME capacitors fired with conventional and microwave methods.

microwave sintering of BME MLCCs could be accomplished at lower temperature and in a shorter heating time. The peak sintering temperature in the microwave sintering was lowered by 100°C, and heating time by 90%, indicating that the sintering kinetics was substantially enhanced in microwave sintering. In addition, microwave sintering could be carried out in an atmosphere of higher pO_2. In conclusion, microwave sintering can produce components with high levels of performance within the small batch firings studied here. It is clear that microwave sintering on larger kilns for large-scale production is an important arena of study in the near future.

4. Summary

Microwave sintering of Ni-electrode MLCCs was conducted in an intermediate reducing atmosphere ∼$pO_2 \times 10^{-6}$ atm. It was found that in the temperature range

Table 2. Comparison of microwave and conventional sintering of BME MLCCs.

Process	°C/min	Heating (h)	Atmosphere	pO$_2$ (atm)	*Density	Properties
Conventional	2	15	Wet/flow	10^{-9}	5.74	Control
Microwave	20–25	1.5–2.0	Dry/static	10^{-6}	5.7–5.8	Comparable

*Geometric density of the as-sintered samples.

around 1250°C, the X7R 0603 MLCC chips were sintered well, resulting in dense and uniform parts without any delaminations or cracks. The dielectric properties of the microwave-sintered BME MLCCs were comparable to the standard products sintered by conventional process. A selected batch of microwave-sintered BME MLCCs passed HALT.

Compared to the conventional process, the microwave sintering conducted in a dry and static atmosphere, with a heating rate one order of magnitude higher, heating time one order of magnitude shorter, and sintering temperature 100°C lower than the conventional process, produced MLCC parts of similar quality and saved about 90% in processing time. The advantages of microwave process for the application of MLCCs are significant.

Acknowledgments

References

1. Yukio Sakabe, in *Ceramic Transactions*, Vol. 97, *Multilayer Electronic Ceramic Devices*, edited by J.-H. Jean, T.K. Gupta, K.M. Nair and K. Niwa (Am. Ceram. Soc., 1999) p 3.
2. T. Nomura and Y. Nakano, in *Ceramic Transactions*, Vol. 131, *Recent Developments in Electronic Materials and Devices*, edited by. K.M. Nair, A.S. Bhalla and S.I. Hirano (Am. Ceram. Soc., Westerville, OH, 2002) p. 87.
3. H. Kishi, Y. Mizuno, and H. Chazono, *Jpn. J. Appl. Phys.* **42**(1), 1 (2003).
4. C.A. Randall, *J. Ceram. Soc. Jap.*, **109**(1), 52 (2001).
5. M.R. Optiz, K. Albertson, J.J. Beeson, P.F. Hennings, J.L. Roubert, and C.A. Randall, **86**(11), 1879 (2003).
6. G.Y. Yang, E.C. Dickey and C.A. Randall, *J. Appl. Phys.* (Submitted).
7. G.Y. Yang, G.D. Lian, E.C. Dickey and C.A. Randall, *J. Appl. Phys.* (Submitted).
8. B.S. Rawal and M. Kahn, *Adv. in Ceramics*, **1**, 48 (1981).
9. C.A. Randall, S.F. Wang, D. Laubscher, J. Dougherty, and W. Huebner, *J. Mat. Res.*, **8**(4), 871 (1993).
10. H. Chazono and H. Kishi, *Jpn. J. Appl. Phys.* **40**, 5624 (2001).
11. Y. Tsur, T.D. Dunbar, and C.A. Randall, *J. Electroceramics*, **7**(1), 25 (2001).
12. Y. Tsur, A. Hitomi, I. Scrymgeour, and C.A. Randall, *Jap. J. Appl. Phys.*, **40**(1), 225 (2001).
13. T. Dunbar, W.L. Warran, B.A. Tuttle, C.A. Randall, and Y. Tsur, *J. Phys. Chem. B*, **108**(3), 908 (2004).
14. W.H. Sutton, *Am. Ceram. Soc. Bull.*, **68**(2), 376 (1989).
15. R. Roy, S. Komarneni, and L.J. Yang, *J. Am. Ceram. Soc.*, **68**(7), 392 (1985).
16. J.D. Katz, *Annu. Rev. Mater. Sci.*, **22**, 153 (1992).
17. D.E. Clark, D.C. Folz, and J.K. West, *Mater. Sci. Engng.*, **A287** 153 (2000).
18. Y. Fang, D.K. Agrawal, W. Hackenberger, T.R. Shrout, and R. Roy, *J. Am. Ceram. Soc.* (submitted)
19. H. Saita, Y. Fang, A. Nakano, D.K. Agrawal, M.T. Lanagan, T.R. Shrout, and C.A. Randall, *Jpn. J. Appl. Phys.*, **41**, 86 (2002).
20. R.J. Lauf, C.E. Holcombe, and C. Hamby, in *Microwave Processing of Materials III*, edited by R.L. Beatty, W.H. Sutton, and M.F. Iskander, in *MRS Symposium Proceedings* (MRS, Pittsburgh, PA), Vol. 269, 1992, pp. 223–229.
21. Y. Fang, D.K. Agrawal, M.T. Lanagan, T.R. Shrout, C.A. Randall, M. Randall, and A. Henderson, in *Ceram. Trans.*, (Am. Ceram. Soc., Westerville, OH, 2004), Vol. 150, p. 359.
22. Y. Fang, H. Peng, D. Agrawal, M.T. Lanagan, C.A. Randall, and M. Randall, "Microwave Co-firing of Base-Metal-Electrode Multilayer Capacitors," presentation at ICE 2003, at MIT, MA, USA, paper number OS2-MLC-6-O, see Abstract Book, p. 75.